Unveiling the Roles of Low-Density Lipoprotein Receptor-Related Protein 6 in Intestinal Homeostasis, Regeneration and Oncogenesis

Jennifer Raisch
Université de Sherbrooke
Anthony Côté-Biron
Université de Sherbrooke
Marie-Josée Langlois
Université de Sherbrooke
Caroline Leblanc
Université de Sherbrooke
Nathalie Rivard (Nathalie.Rivard@USherbrooke.ca)
Université de Sherbrooke

Research Article

Keywords: LRP6, intestine, stem cells, regeneration, inflammation, colorectal cancer.

Posted Date: February 22nd, 2021

DOI: https://doi.org/10.21203/rs.3.rs-199544/v1

Unveiling the roles of Low-Density Lipoprotein Receptor-Related Protein 6 in intestinal homeostasis, regeneration and oncogenesis.

Jennifer Raisch[1], Anthony Côté-Biron[1], Marie-Josée Langlois[1], Caroline Leblanc[1], Nathalie Rivard[1*]

[1]Department of Immunology and Cell Biology, Cancer Research Pavilion, Faculty of Medicine and Health Sciences, Université de Sherbrooke, Sherbrooke, Canada.

Short Title: LRP6 controls intestinal stem cell functionality and BRAF-mediated oncogenesis

[*]Corresponding author
3201, Jean-Mignault
Sherbrooke, QC
Canada
J1E4K8
Email: Nathalie.Rivard@USherbrooke.ca
Phone: 819-821-8000 (75943)

Abstract

Intestinal epithelial self-renewal is tightly regulated by signaling pathways controlling stem cell proliferation, determination and differentiation. In particular, Wnt/β-catenin signaling controls crypt cell division and survival and is required for maintenance of the intestinal stem cell niche. Most colorectal cancers are also initiated by mutations activating the Wnt/β-catenin pathway. Wnt signals are transduced through Frizzled receptors and LRP5/LRP6 coreceptors to downregulate GSK3β activity, resulting in increased nuclear β-catenin. Herein, we explored if LRP6 expression is required for maintenance of intestinal homeostasis, regeneration and oncogenesis. Mice with an intestinal epithelial cell-specific deletion of *Lrp6* (*Lrp6*$^{IEC\text{-}KO}$) were generated and their phenotype analyzed. No difference in intestinal architecture or in proliferative and stem cell numbers was found in *Lrp6*$^{IEC\text{-}KO}$ mice in comparison to controls. Nevertheless, using *ex vivo* intestinal organoid cultures, we found that LRP6 expression was critical for crypt cell proliferation and stem cell maintenance. When exposed to dextran sodium sulfate, *Lrp6*$^{IEC\text{-}KO}$ mice developed more severe colitis than control mice. However, loss of LRP6 did not affect tumorigenesis in *Apc*$^{Min/+}$ mice nor growth of human colorectal cancer cells. By contrast, *Lrp6* silencing diminished anchorage-independent growth of *BRaf*^{V600E}-transformed IEC. Thus, LRP6 controls intestinal stem cell functionality and is necessary for BRAF-induced IEC oncogenesis.

.

Key words: LRP6, intestine, stem cells, regeneration, inflammation, colorectal cancer.

Introduction

Intestinal stem cells, located at the base of intestinal crypts, play a central role in the establishment and maintenance of the intestinal epithelium. These cells undergo asymmetric division leading to migration and differentiation along the intestinal crypt axis [1]. Thus, the intestinal epithelium self-renewal is tightly regulated by interacting intracellular signaling pathways controlling stem and progenitor cell expansion and differentiation [2]. In particular, the Wnt/β-catenin pathway controls proliferation and survival and is required for the maintenance of intestinal stem cells. Wnt factors signals through Frizzled receptors and LRP5/LRP6 coreceptors to downregulate Glycogen Synthase Kinase 3β (GSK3β) activity, resulting in increased nuclear β-catenin [3–5]. In the absence of Wnt ligand, β-catenin is destabilized by a destruction complex composed of casein kinase 1 alpha (CK1α), GSK3β, Axin and adenomatous polyposis coli (APC) proteins. β-catenin binds to the destruction complex and is phosphorylated by CK1α and then by GSK3β, which marks β-catenin for ubiquitin-mediated degradation by the proteasome [3,5]. Wnt and its receptor then form a trimeric complex with plasma membrane-associated LRP5/LRP6. This trimeric complex recruits the scaffold protein Dishevelled (DVl) which itself polymerizes and recruits Axin inducing LRP5/LRP6 aggregation. These aggregates, named signalosomes, promote phosphorylation of LRP5/LRP6 by CK1γ and GSK3β, releasing β-catenin. β-catenin then accumulates into the cytosol and translocates into the nucleus to interact with nuclear DNA-binding T-cell factor (TCF) and lymphoid enhancer-binding protein (LEF), forming a functional transcription factor promoting target gene expression.

LRP6 is a type I single-span transmembrane protein with 1613 amino acid residues organized in a long extracellular domain, a transmembrane domain and a short intracellular domain necessary for signaling activity [6]. The extracellular domain is divided into 4 sub-domains (E1-E4), each composed of YWTD β-propeller and EGF-like motifs involved in ligand recognition. Mice lacking LRP6 die at birth, indicating that LRP6 plays a crucial role in tissue development and homeostasis [7,8]. Nevertheless, the phenotype of *Lrp6*$^{-/-}$ mice is less severe than the phenotype observed in mice mutated for Wnt ligands, possibly because of the compensatory action triggered by its closely related paralog LRP5, as observed during intestinal development in mice [9].

Most colorectal cancers (CRC) are initiated by mutations activating the Wnt/β-catenin pathway, commonly in the *APC* gene [10]. LRP6 expression and phosphorylation are increased in sporadic CRC tumors [11–13]. Increased LRP6 phosphorylation correlates with tumour malignancy and staging as well as with poor prognosis, suggesting an important contribution of LRP6 activation in CRC development and disease outcome [13]. Interestingly, LRP6 is phosphorylated on serine-1490 and threonine-1572 in a MEK-dependent manner in rodent IEC transformed by oncogenic KRAS and BRAF[11]. These results suggest that LRP6 phosphorylation may be involved in human colorectal carcinogenesis induced by oncogenic KRAS and BRAF signaling.

Herein, we analyzed the role of LRP6 in intestinal epithelial homeostasis, inflammation and oncogenesis. We show that LRP6 is required to maintain the regenerative abilities of intestinal stem cells, thereby protecting the murine epithelium against DSS-induced mucosal damage and inflammation. As expected, LRP6 is dispensable for adenoma formation in $Apc^{Min/+}$ mice and for growth of human CRC cells in culture. However, LRP6 is hyperphosphorylated in KRAS and BRAF-mutated human CRC cells and important for growth of $BRaf^{V600E}$-transformed IEC.

Results

Lrp6 deletion does not alter intestinal architecture and homeostasis but impairs Wnt target gene expression.

To address the importance of LRP6 in intestinal development and architecture, we bred *Lrp6*$^{loxP/loxP}$ mice with *Villin*-Cre mice that express the Cre recombinase in intestinal epithelial cells [14] leading to specific loss of LRP6 expression in these cells (Fig. 1a). Because LRP6 is a co-receptor involved in the activation of the Wnt/β-catenin signaling pathway, we verified the activation status of this pathway by analyzing the levels of total and activated β-catenin protein. As shown in Fig. 1a, total and active β-catenin levels were not significantly different in mutant and control mucosae. Although we did not observe a difference in β-catenin expression levels, we cannot exclude that subtle changes might occur in its transcriptional activity. We therefore analyzed the expression levels of Wnt/β-catenin target genes. Intriguingly, while *Cd44*, *Sox9* and *Ascl2* gene expression remained unaffected by loss of epithelial LRP6, *Axin2*, *Lgr5* and *EphB3* gene expression was significantly decreased in *Lrp6*$^{IEC-KO}$ mucosal enrichments (Fig. 1b). Histological analyses of *Lrp6*$^{IEC-KO}$ mouse jejunal sections revealed, however, no difference in intestinal architecture, villus length, crypt depth and proliferation in comparison to control littermates (Fig. 1c and d). No histological change was observed in the colonic epithelium as well (Fig. S1). Expression levels of genes encoding mucin 2, lysozyme and sucrase-isomaltase, the main markers of respectively goblet, Paneth and absorptive differentiated cells, were also comparable between control and mutant mice (Fig. 1e). The decreased expression of *Lgr5* in *Lrp6* KO mucosal enrichments suggests a change in the number of active cycling stem cells, also named crypt base columnar (CBC) cells. We therefore performed immunofluorescence against OLFM4, a robust marker for these cells. As shown in Fig. 1f, similar numbers of OLFM4-positive cells were found in *Lrp6*$^{IEC-KO}$ and control mice. Thus, while loss of LRP6 in intestinal epithelial cells reduced the expression of some Wnt target genes, including the stem cell marker *Lgr5*, it was not sufficient to perturb homeostatic maintenance of the intestinal epithelium under normal conditions.

LRP6 expression is required for *ex vivo* intestinal crypt regeneration.

Since the expression of some Wnt target genes is reduced upon *Lrp6* deletion, we next examined regenerative abilities of intestinal stem cells by preparing enteroids from control and *Lrp6*$^{IEC-KO}$ mice [15]. Notably, development of *Lrp6*$^{IEC-KO}$ enteroids was clearly compromised in comparison to

control enteroids. Indeed, the number of protrusions was significantly reduced in enteroids lacking *Lrp6* expression (Fig. 2a). Three days after seeding, proliferation of *Lrp6*-deficient enteroids was significantly decreased in comparison to control enteroids as visualized by reduced number of EdU-positive cells (Fig. 2b). After 5 days, *Lrp6*-deficient enteroids degenerated and died (Fig. 2c) and increased expression of the pro-apoptotic *Noxa* gene was noticed (Fig. 2d). To examine the effect of *Lrp6* deletion on Wnt signaling in enteroids, we determined the mRNA expression level of Wnt target stem cell genes by quantitative RT-PCR. There was a significant reduction in the expression of *Axin2*, *Lgr5*, *Ascl2*, *and Cd44* in *Lrp6*$^{\text{IEC-KO}}$ enteroids, 3 days after seeding (Fig. 2e and f). Thus, loss of *Lrp6* expression disrupts *ex vivo* intestinal stem cell renewal and crypt regeneration.

Lrp6$^{\text{IEC-KO}}$ mice are more sensitive to DSS-induced epithelial damage and colitis.

We next evaluated the susceptibility of control and *Lrp6*$^{\text{IEC-KO}}$ mice to develop colonic inflammation in response to dextran sodium sulfate (DSS) administration. As shown in Figure 3a-c, after 7 days, DSS administration induced acute colitis in control mice, as shown by significant weight loss, diarrhea and occasional bleeding resulting in a relatively high Disease Activity Index (DAI). Interestingly, *Lrp6*$^{\text{IEC-KO}}$ mice exhibited more weight loss (Fig. 3a) and significantly higher DAI associated with more severe diarrhea, rectal bleeding and bloody stools (Fig. 3b). Hematoxylin and eosin staining was also performed on colonic tissue to score damage according to the extent of destruction of the mucosal architecture, the presence of cellular infiltration, crypt abscesses, goblet cell depletion and the extent of muscle thickening, all typical alterations observed during colitis (Fig. 3d). As shown in Fig. 3c, *Lrp6*$^{\text{IEC-KO}}$ mice exhibited a significantly higher histological score than control mice, indicating that *Lrp6*$^{\text{IEC-KO}}$ intestinal mucosa was more affected following DSS treatment.

LRP6 is dispensable for adenoma formation in _Apc_$^{\text{Min/+}}$ mice and for growth of human colorectal cancer cells.

Because initiation of most colorectal cancers (CRC) is often due to activating mutations in Wnt/β-catenin signaling, we verified the role of LRP6 in *Apc*$^{\text{Min/+}}$ mice which are heterozygous for an *Apc* mutation frequently found in human CRC, and which spontaneously develop intestinal adenomas [16]. *Lrp6*$^{\text{IEC-KO}}$ mice were crossed with *Apc*$^{\text{Min/+}}$ mice and intestinal tumour load was analyzed after

3 months. Unexpectedly, the absence of LRP6 did not significantly affect tumor development in *Apc*$^{Min/+}$ mice (Fig. 4a and b). We next assessed the role of LRP6 in two established human CRC cell lines exhibiting activated Wnt signaling, namely HCT116 (*CTNNB1* mutation) and SW48 (*APC* mutation) cells, by using a doxycycline-inducible shRNA expression vector targeting *LRP6* mRNA, to knockdown LRP6 protein expression. As shown in Figure 4c, LRP6 protein levels were significantly reduced by 67% in HCT116 cells and by 69% in SW48 cells following doxycycline addition. However, this decrease in LRP6 expression was not sufficient to alter clonogenic potential nor anchorage-independent growth (Fig. 4d-f).

ERK-dependent phosphorylation of LRP6 in *KRAS* and *BRAF*-mutated colorectal cancer cells – a role for LRP6 in BRAF-induced intestinal oncogenesis.

Previously, we reported that oncogenic KRAS and BRAF signaling in rodent intestinal epithelial cells (IEC-6 cells) activates the canonical Wnt/β-catenin pathway by increasing LRP6 phosphorylation [11]. Accordingly, treatment of *KRAS* (HCT116) and *BRAF* (HT-29)-mutated human CRC cells with the ERK1/2 inhibitor, SCH7729846, reduced LRP6 phosphorylation on serine 1490, a residue localized within one of the PPPS/TP motifs required for Wnt signal transduction. Interestingly, LRP6 phosphorylation was not or only barely affected by the SCH7729846 inhibitor in *KRAS* and *BRAF* wild-type CRC cells (Caco-215 or SW48) (Fig. 5a). These data suggest that LRP6 phosphorylation may be instrumental for oncogenesis induced by abnormal ERK signaling. We therefore knocked down LRP6 expression in IEC-6 cells transformed by the 4-hydroxytamoxifen-inducible BRAF^{V600E}:ER fusion protein (Fig. 5b). As shown in Fig. 5c, LRP6 silencing clearly reduced the ability of oncogenic BRAF to induce anchorage-independent growth in IEC-6 cells.

Discussion

Although LRP6 is involved in Wnt/β-catenin signaling transduction, its role in the maintenance of intestinal homeostasis remains unclear [9]. Herein, we demonstrated that IEC-specific *Lrp6* deletion in mice does not affect intestinal development nor crypt cell proliferation and differentiation. Because the maintenance of Wnt signaling in the intestinal epithelium is absolutely required to maintain homeostasis, total and active β-catenin expression was first analyzed as a readout of Wnt pathway activation. Importantly, levels of total and active β-catenin proteins remained similar between control and *Lrp6*-deficient mucosae. Nonetheless, expression of some Wnt target genes, namely *Lgr5*, *Axin2* and *Ephb3*, was significantly decreased in *Lrp6*$^{\text{IEC-KO}}$ mice, suggesting that intestinal crypt cells might be somehow less responsive to Wnt stimulation in absence of the LRP6 protein. One of the reduced genes, *Lgr5*, was previously recognized as a marker of active cycling stem cells, located at the crypt base of the crypt-villus axis, and whose self-renewal is dependent on Wnt signaling. Hence, impaired activation of Wnt pathway activation may result in decreased LGR5-positive active stem cell numbers as observed after β-catenin deletion in the murine intestinal epithelium [17]. However, immunofluorescence against OLFM4 protein, a robust marker for these stem cells [18], indicates that *Lrp6*$^{\text{IEC-KO}}$ and control crypts retain similar numbers of active stem cells. Additionally, expression of *Ascl2*, a Wnt-responsive master transcription factor that controls LGR5-positive intestinal stem cell gene expression programs [19], remains unaffected without LRP6 in the murine intestinal epithelium. Thus, although *Lgr5* gene expression is reduced, the number of active cycling stem cells and proliferative cells in *Lrp6*-deficient crypts remain comparable to what is observed in control crypts. This could be at least explained by the fact that LRP5, a LRP6 ortholog, is also expressed in murine crypt epithelial cells [20]. Indeed, LRP5 and LRP6 play compensatory functions during intestinal epithelial development in mice [9]. A modest increase in LRP5 protein expression was observed in *Lrp6*$^{\text{IEC-KO}}$ intestines in comparison to controls (Fig. S2a). This slight LRP5 increase could be sufficient to sustain enough Wnt signaling and maintain intestinal homeostasis and renewal in mice.

Interestingly, *Lrp6*$^{\text{IEC-KO}}$ jejunal crypt enteroids showed hindered proliferation and died a few days after seeding, probably by increased apoptosis, as suggested by the increased expression of the pro-apoptotic gene *Noxa*. Decreased *Lrp6*-deficient enteroid proliferation and viability may be due to

Wnt signaling inhibition in stem and progenitor cells, as revealed by the substantial decreased expression of the Wnt target genes *Lgr5*, *Ascl2*, *Axin2* and *CD44*. Additionally, *Olfm4* was also significantly decreased in *Lrp6*-deficient enteroids. Decreased expression of *Olfm4*, *Ascl2* and *Lgr5* strongly indicates that functionality of active stem cells in enteroids was impaired in the absence of LRP6. Since such alterations were not observed *in vivo*, one could speculate that underlying mesenchymal niche cells likely maintain stem cell homeostasis in *Lrp6*$^{\text{IEC-KO}}$ mice, certainly through LRP5 activation. Moreover, our findings are reminiscent of those observed with *Math1*- and *Wnt3*-inducible-IEC-KO mouse models. While no alteration in stem cell numbers and Wnt signaling, as assessed by measuring active β-catenin levels, was observed *in vivo*, enteroids derived from these KO mice could not grow [21,22]. Of note, MATH1 is an essential driver of differentiation of secretory cells including Paneth cells which produce growth factors such as epidermal growth factor, Notch and Wnt3 which collectively promote growth and maintenance of LGR5-positive stem cells. Therefore, the absence of MATH1 specifically in intestinal epithelial cells, leads to crypt enteroid growth arrest, resulting from the inhibition of Paneth cell differentiation and of the production of growth factors, especially Wnt3 [22]. Thus, these studies have revealed that Paneth cell-secreted Wnt3 is not the only niche factor involved in stem cell maintenance in vivo, suggesting that redundant Wnt signals exist in mice to insure intestinal homeostasis. Indeed, intestinal stromal cells act as important regulators of the stem cell niche, by producing and secreting several Wnt factors, notably Wnt2b and Wnt4 [23–27]. Although *Wnt2b* or *Wnt4* gene expression was not modulated in *Lrp6*$^{\text{IEC-KO}}$ intestines, other mesenchymal-derived Wnt factors may contribute to the maintenance of intestinal homeostasis in *Lrp6*$^{\text{IEC-KO}}$ mice (Fig. S2b).

A variant of the human *LRP6* gene was recently found to be frequently expressed in early onset ileal Crohn's Disease, a chronic intestinal inflammatory disorder [28]. We therefore analyzed the sensitivity of *Lrp6*$^{\text{IEC-KO}}$ mice to intestinal inflammation. DSS-treated *Lrp6*$^{\text{IEC-KO}}$ mice displayed increased DAI and more severe mucosal histological damage than control mice. The mechanisms explaining this increased susceptibility to develop colitis in the absence of *Lrp6* still need to be determined. However, although LRP6 was dispensable for the maintenance of intestinal homeostasis under homeostatic conditions, our data suggest that LRP6 may be important to insure adequate intestinal mucosal recovery through crypt regeneration, following epithelial damage. Indeed, histological analysis of *Lrp6*-deficient colonic mucosae after DSS treatment revealed the

presence of large areas still denuded of epithelium, as opposed to DSS-treated control mice. Increased epithelial cell proliferation is necessary to allow intestinal mucosal recovery after DSS-induced injury [29]. In this regard, IBD patient mucosa exhibits enhanced epithelial proliferation, which decreases during resolution of inflammation [30]. Altogether, these data suggest that, by promoting crypt regeneration, LRP6 may protect the intestinal epithelium against damage and inflammation.

Most CRC develop via adenomatous polyps initiated by mutations activating the Wnt/β-catenin pathway, commonly in the adenomatous polyposis coli *(APC)* gene or less frequently in the β-catenin (*CTNNB1*) gene. Interestingly, LRP6 overexpression in CRC cells activates Wnt/β-catenin signaling and cell migration [13]. However, whether LRP6 expression contributes to Wnt signaling and CRC tumoral properties, especially in CRC with *APC* or β-catenin mutations, remains unclear. Chen and He (2019) did not observe changes in Wnt signaling activation in APC-deficient CRC cells after *Lrp6* knockout by CRISPR/Cas9 genome editing [31]. In contrast, Saito-Diaz *et al*. (2018) demonstrated that LRP6 knockdown in CRC cells, even those exhibiting *APC* mutations, significantly reduced Wnt signaling [32] and this was recently confirmed by single cell analyses of endogenous β-catenin levels [33]. Unfortunately, in their study, Saito-Diaz et al. (2018) did not analyze the impact of LRP6 knockdown on CRC cell growth. Herein, we show that decreasing LRP6 expression by 65-70% did not affect CRC cell clonogenic potential nor ability to form colonies in soft agar. Of note, the two cell lines analyzed, namely HCT116 and SW48 cells, exhibit mutations in respectively *CTNNB1* (β-catenin) and *APC* genes. Thus, our results suggest that CRC cells harboring activating mutations in Wnt signaling do not need LRP6 expression for their growth. Likewise, epithelial *Lrp6* deletion does not affect intestinal tumor load and size in $Apc^{Min/+}$ mice. Taken together, these findings support the notion that epithelial LRP6 expression is dispensable not only for the maintenance of intestinal homeostasis but also for tumorigenesis induced by aberrant β-catenin signaling.

Serrated adenocarcinomas, which account for 20-30% of CRC, follow an alternative pathway independent of *APC* mutations, in which serrated polyps replace traditional adenoma as the CRC precursor lesion [34]. This pathway involves early *BRAF* mutations, excess CpG island methylation and DNA microsatellite instability (MSI). Previous reports have demonstrated that expression of

constitutively active mutants of BRAF or KRAS in non-transformed IEC, such as IEC-6 cells, is sufficient to promote tumoral transformation [11,35]. We previously reported that expression of $BRAF^{V600E}$ or $KRAS^{G12D}$ oncogenes in IEC activates β-catenin nuclear transcriptional activity and target gene expression [11]. Notably, LRP6 was phosphorylated on serine-1490 and threonine-1572 in a MEK-dependent manner, in IEC transformed by oncogenic KRAS or BRAF, thus providing a mechanism integrating KRAS/MAPK and canonical Wnt/β-catenin signaling during intestinal transformation. Indeed, both the serine-1490 and threonine-1572 residues are localized within the PPPS/TP motifs of the LRP6 co-receptor, motifs required for Wnt signal transduction. Herein, we observed ERK-dependent LRP6 phosphorylation in human CRC cell lines with *KRAS* or *BRAF* mutations. This suggests that LRP6 phosphorylation is involved in oncogenic signaling induced by *KRAS* or *BRAF* mutations. However, LRP6 silencing in HCT116 cells which harbor *KRAS* mutation did not significantly alter anchorage-independent growth nor clonogenic potential. It is important to note that in addition to *KRAS* mutation, HCT116 cells exhibit several other genetic alterations including *PIK3CA* mutation, CIMP and microsatellite instability that may also stimulate their growth. To circumvent this situation, we have used a simpler model, namely IEC-6 stably expressing an inducible oncogenic form of human BRAF, $BRAF^{V600E}$:ER. Following stimulation with 4-hydroxytamoxifen, $BRAF^{V600E}$ induced ERK1/2 signaling, cell transformation and anchorage-independent growth [35]. LRP6 knockdown in this model significantly reduced the capacity of $BRAF^{V600E}$ to induce colony formation in soft agar, which is a measure of anchorage-independent growth potential correlating with tumorigenic growth *in vivo*.

In conclusion, although LRP6 does not play an essential role in the regulation of intestinal homeostasis and *Apc*-induced tumorigenesis in mice, LRP6 promotes crypt regeneration after epithelium damage and contributes to oncogenesis induced by BRAF oncogene. Our results suggest that LRP6 could represent a novel target for colorectal tumorigenesis associated with *KRAS* or *BRAF* mutations.

Methods

Antibodies and reagents

Primary antibodies were obtained from the following sources: β-actin (MAB1501R) from Millipore (Oakville, Canada), ERK2 (sc-154) from Santa Cruz Biotechnology (Santa Cruz, CA, USA), phosphorylated ERK1/2 (M8159) from Sigma-Aldrich (Oakville, ON, Canada), non-phospho (active) β-catenin (D13A1), LRP5 (D80F2), LRP6 (C5C7), LRP6 (C47E12), phospho-LRP6 (Ser1490) from Cell Signaling Technology (Danvers, MA, USA) and β-catenin (C14), BrdU (B44) from BD Biosciences (San Jose, CA, USA). Horseradish peroxidase antibodies were obtained from GE Healthcare Life Sciences (Mississauga, ON, Canada) and alkaline phosphatase-conjugated antibodies from Promega (Madison, WI, USA). For immunofluorescence, Alexa Fluor 488 conjugated antibodies were obtained from Molecular Probes (Waltham, MA, USA). The specific ERK inhibitor SCH772984 was bought from Cayman Chemical (Ann Arbor, MI, USA). Other materials were purchased from Sigma-Aldrich unless stated otherwise.

Cell culture

Human CRC cell lines HCT116 (ATCC CCL-247) and HT-29 (ATCC HTB-38) were maintained in McCoy's 5A (Wisent, Saint-Bruno, QC, Canada) supplemented with 5% FBS (Wisent). SW48 (ATCC CCL-231) and Caco-2/15 (obtained from Dr A. Quaroni, Cornell University, Ithaca, NY, USA) cell lines were maintained in DMEM (Wisent) containing 10% FBS. Previously described IEC6 $BRAF^{V600E}$:ER cells [36] were cultured in DMEM without phenol red (Wisent) and supplemented with 5% charcoal stripped FBS (Wisent). Cells were cultured at 37˚C under a humidifying atmosphere containing 5% CO_2.

Mice

The C57BL/6 12.4KbVilCre transgenic mouse line was provided by D. Gumucio (University of Michigan, Ann Arbor, MI, USA). These mice were crossed with *Lrp6*$^{loxP/loxP}$ mice purchased from Jackson Laboratory to generate conditional knockout mice with a specific deletion of the *Lrp6* gene in intestinal epithelial cells. Mutant mice or *Lrp6*$^{loxP/loxP}$;Villin-Cre mice (*Lrp6*$^{IEC\text{-}KO}$ mice) were compared to control mice (*Lrp6*$^{loxP/+}$ or *Lrp6*$^{loxP/loxP}$). C57BL6/J-*Apc*$^{Min/+}$ mice were purchased from Jackson Laboratory. For tumor initiation experiments, *Lrp6*$^{loxP/loxP}$;*Villin*-Cre;*Apc*$^{Min/+}$ mice were

compared to *Lrp6*$^{loxP/+}$;*Apc*$^{Min/+}$ or *Lrp6*$^{loxP/loxP}$;*Apc*$^{Min/+}$ control mice. Genomic DNA was extracted from tissue by digestion in 25 mM NaOH/0.2 mM EDTA heated at 95°C for 1 h followed by addition of an equal volume of 40 mM Tris-HCl (pH 5.5). PCR conditions and primer sequences used for genotyping are available upon request. All experiments were approved by the Animal Research Ethics Committee of the Université de Sherbrooke (committee approval number FMSS-399-18B) in accordance with the Canadian Council on Animal Care standards.

Colitis induction with DSS and clinical evaluation

Ten to twelve-week-old *Lrp6*$^{IEC-KO}$ mice and their control littermates were administered dextran sodium sulfate 1.75-2% (DSS, colitis grade; MP Biomedical, Solon, OH, USA) in drinking water ad libitum for 7 days. Clinical parameters such as weight loss, rectal bleeding and diarrhea were monitored every day. The disease activity index (DAI) was measured at day 7 according to Cooper *et al.* [37]. Histological damage scoring was assessed on hematoxylin and eosin-stained sections based on the destruction of normal mucosal architecture (0, normal; 1, 2, and 3, respectively, mild, moderate, and extensive damage), presence and degree of cellular infiltration (0, normal; 1, 2, and 3, respectively mild, moderate, and transmural infiltration), extent of muscle thickening (0, normal; 1, 2, and 3, respectively mild, moderate, and extensive thickening), presence or absence of crypt abscesses (0, absent; 1, present) and the presence or absence of goblet cell depletion (0, absent; 1, present). All clinical scorings were performed in a blinded manner.

Macroadenoma count, histological staining, immunofluorescence, and immunohistochemistry

Polyps were stained with methylene blue and visualized under an SZ51 stereomicroscope (Olympus, Richmond Hill, Canada). Polyp sizes were measured with a digital caliper (Thermo Fisher Scientific, Waltham, MA, USA) and polyp numbers were counted from the duodenum to the rectum as described previously [38]. For BrdU staining, mice were injected with BrdU (10 µl/g of body weight; Thermo Fisher Scientific (Invitrogen)) 90 min before sacrifice. Tissues were fixed with paraformaldehyde 4%, paraffin embedded, sectioned and stained as described before [39]. Immunohistochemistry staining was performed with Dako EnVision+System Kit (Dako, Santa Clara, CA, USA) according to the manufacturer's protocol. Slides were visualized with a

NanoZoomer slide scanner and NDP.view2 software (Hamamatsu, Boston, MA, USA). All cell counts were performed on well-oriented crypts in a blinded manner.

Enteroids

Crypts were isolated from the jejunum of 8 to 12-week-old mice with 30 mM EDTA, as described previously [40]. Enteroids were cultured and passaged as described [41]. Phase-contrast images were taken using a Zeiss Celldiscoverer 7 live Imaging Station equipped with ZEN software (Carl Zeiss, Toronto, ON, Canada). Proliferation was evaluated in enteroid culture using the Click-it 5-Ethynyl-2′-deoxyuridine (EdU) Alexa Fluor 555 imaging kit (Thermo Fisher Scientific) according to the manufacturer's instructions and visualized by confocal microscopy (LSM Olympus FV1000 apparatus and FV10-ASW 3.1 software; Olympus; Center Valley, PA, USA).

Western blot analysis

Proteins from scraped intestinal mucosa enrichments were isolated in chilled RIPA buffer. Proteins from cell lines were extracted in chilled Triton X-100 buffer. After an incubation of 30 min upon agitation, samples were sonicated (15%, 10 sec). Protein quantification was performed using Pierce™ BCA protein assay (Thermo Fisher Scientific). Protein extracts were finally diluted in Laemmli buffer [62.5 mM Tris-HCl (pH 6.9), 2% sodium dodecyl sulfate, 1% β-mercaptoethanol, 10% glycerol, and 0.04% bromophenol blue] before processing for western blot analysis.

RNA extraction and qRT–PCR

RNA was isolated from the scraped jejunum mucosa of mice and from enteroids using the RNeasy minikit including on-column DNase digestion (Qiagen). RT-PCR was performed using the Transcriptor reverse transcriptase with random hexamer primers (Roche Diagnostics). Quantitative polymerase chain reaction (qPCR) was performed by the RNomics Platform at the Université de Sherbrooke. Target expression was quantified relatively to *Pum1*, *Psmc4*, and *Tbp* expression. PCR conditions and primer sequences are available upon request.

LRP6 silencing

To silence LRP6 expression in human colorectal cancer cell lines, we used inducible small hairpin RNA (shRNA) plasmids containing 21-mer shRNA sequences targeting the human *LRP6* gene.

The plasmid backbone Tet-pLKO-puro was provided by Dmitri Wiederschain (Addgene plasmid #21915) [42]. Noneffective 21-mer-non-target shRNA previously described [43] was a gift from Pr François Boudreau and was used as a control. Stable cell line populations were generated as previously described [11]. ShRNA expression was induced in appropriate medium containing 50 ng/ml doxycycline. To silence LRP6 expression in IEC6 $BRAF^{V600E}$:ER cells, we used small hairpin RNA (shRNA) plasmids containing 29-mer shRNA sequences in a green fluorescent protein (GFP) vector targeting the rat *Lrp6* gene as previously described [11]. A noneffective 29-mer-scrambled shRNA cassette in pGFP-V-RS Vector (Origene, Rockville, MD, USA) was used as control. IEC6 $BRAF^{V600E}$:ER cells were infected with either control or *Lrp6*-shRNA lentiviruses. After selection with puromycin (1 μg/ml), cells were used for further studies.

Soft agar assay

Inducible shRNA cell lines were treated with 50 ng/ml doxycycline 48 h before seeding. Cells were counted using a hemocytometer and approximately 30 000 (SW48) or 10 000 cells (HCT116) were seeded in 0,7% agarose prepared by mixing pre-warmed media 1:1 with autoclaved 1.4% agarose type VII as previously described [44]. Media containing 50 ng/ml doxycycline and 10% FBS were changed every 48 h. Untransfected or shRNA expressing IEC6 $BRAF^{V600E}$:ER cells were treated with 250 nM 4OH-Tamoxifen (Cayman, Ann Arbor, MI, USA) 16 h before seeding 30 000 cells per well in 0,7% agarose type VII. Media containing 250 nM 4OH-Tamoxifen were changed every 48 h. Cells were grown for 14 (HCT116), 21 (SW48) or between 21-35 days for IEC6 $BRAF^{V600E}$:ER cells. Colonies were then stained with 0,5 mg/ml MTT (3-(4,5-dimethylthiazol-2-yl)-2,5-diphenyltetrazolium bromide) dissolved in the appropriate medium for 4 h at 37°C and 5% CO_2. Images were acquired using an Infinity VX2 1100/26MX Imaging System (Vilber Lourmat, Marne-la-Vallée, France). Colonies were counted and their size assessed using ImageJ software (National Institutes of Health, Bethesda, MD, USA).

Clonogenic assay

Inducible shRNA cell lines were treated with 50 ng/ml doxycycline 48 h before seeding. Cells were counted using a hemocytometer and approximately 1000 cells were seeded into six-well plates. Media containing 50 ng/ml doxycycline were changed every 48 h and cells were grown for 14 days. Plates were then stained with a staining solution (0,05% crystal violet, 1% formaldehyde and

1% methanol in PBS). Phase-contrast images were taken using a Zeiss Celldiscoverer 7 live Imaging Station equipped with ZEN software. Colonies were counted using ImageJ software.

Statistical analyses

All assays were carried out at least in triplicate. Typical results shown are representative of three independent experiments if not stated otherwise. Results were analyzed using Student's t-test with populations that followed a normal curve or Mann-Whitney U test in other case. Results were considered statistically significant at $p \leq 0.05$. Graphs and statistics were generated using GraphPad Prism (GraphPad Software, La Jolla, CA, USA).

References

1. Takahashi, T. & Shiraishi, A. Stem Cell Signaling Pathways in the Small Intestine. *Int. J. Mol. Sci.* **21**, 2032 (2020).
2. Tan, S. H. & Barker, N. Chapter Two - Wnt Signaling in Adult Epithelial Stem Cells and Cancer. in *Progress in Molecular Biology and Translational Science* (eds. Larraín, J. & Olivares, G.) vol. 153 21–79 (Academic Press, 2018).
3. Liu, C. *et al.* Control of beta-catenin phosphorylation/degradation by a dual-kinase mechanism. *Cell* **108**, 837–847 (2002).
4. Raisch, J., Côté-Biron, A. & Rivard, N. A Role for the WNT Co-Receptor LRP6 in Pathogenesis and Therapy of Epithelial Cancers. *Cancers* **11**, (2019).
5. Yost, C. *et al.* The axis-inducing activity, stability, and subcellular distribution of beta-catenin is regulated in Xenopus embryos by glycogen synthase kinase 3. *Genes Dev.* **10**, 1443–1454 (1996).
6. Niehrs, C. & Shen, J. Regulation of Lrp6 phosphorylation. *Cell. Mol. Life Sci.* **67**, 2551–2562 (2010).
7. Pinson, K. I., Brennan, J., Monkley, S., Avery, B. J. & Skarnes, W. C. An LDL-receptor-related protein mediates Wnt signalling in mice. *Nature* **407**, 535 (2000).
8. Zhou, C. J. *et al.* Generation of Lrp6 conditional gene-targeting mouse line for modeling and dissecting multiple birth defects/congenital anomalies. *Dev. Dyn.* **239**, 318–326 (2010).
9. Zhong, Z., Baker, J. J., Zylstra-Diegel, C. R. & Williams, B. O. Lrp5 and Lrp6 play compensatory roles in mouse intestinal development. *J. Cell. Biochem.* **113**, 31–38 (2012).
10. Fearon, E. R. & Vogelstein, B. A genetic model for colorectal tumorigenesis. *Cell* **61**, 759–767 (1990).
11. Lemieux, E., Cagnol, S., Beaudry, K., Carrier, J. & Rivard, N. Oncogenic KRAS signalling promotes the Wnt/β-catenin pathway through LRP6 in colorectal cancer. *Oncogene* **34**, 4914–4927 (2015).
12. Rismani, E. *et al.* Pattern of LRP6 gene expression in tumoral tissues of colorectal cancer. *Cancer Biomark. Sect. Dis. Markers* **19**, 151–159 (2017).
13. Yao, Q. *et al.* LRP6 promotes invasion and metastasis of colorectal cancer through cytoskeleton dynamics. *Oncotarget* **8**, 109632–109645 (2017).

14. Madison, B. B. *et al.* Cis elements of the villin gene control expression in restricted domains of the vertical (crypt) and horizontal (duodenum, cecum) axes of the intestine. *J. Biol. Chem.* **277**, 33275–33283 (2002).
15. Drost, J., Artegiani, B. & Clevers, H. The Generation of Organoids for Studying Wnt Signaling. *Methods Mol. Biol. Clifton NJ* **1481**, 141–159 (2016).
16. Moser, A. R., Pitot, H. C. & Dove, W. F. A dominant mutation that predisposes to multiple intestinal neoplasia in the mouse. *Science* **247**, 322–324 (1990).
17. Fevr, T., Robine, S., Louvard, D. & Huelsken, J. Wnt/ -Catenin Is Essential for Intestinal Homeostasis and Maintenance of Intestinal Stem Cells. *Mol. Cell. Biol.* **27**, 7551–7559 (2007).
18. van der Flier, L. G. & Clevers, H. Stem Cells, Self-Renewal, and Differentiation in the Intestinal Epithelium. *Annu. Rev. Physiol.* **71**, 241–260 (2009).
19. Yan, K. S. & Kuo, C. J. Ascl2 reinforces intestinal stem cell identity. *Cell Stem Cell* **16**, 105–106 (2015).
20. Pinto, D., Gregorieff, A., Begthel, H. & Clevers, H. Canonical Wnt signals are essential for homeostasis of the intestinal epithelium. *Genes Dev.* **17**, 1709–1713 (2003).
21. Durand, A. *et al.* Functional intestinal stem cells after Paneth cell ablation induced by the loss of transcription factor Math1 (Atoh1). *Proc. Natl. Acad. Sci.* **109**, 8965–8970 (2012).
22. Farin, H. F., Van Es, J. H. & Clevers, H. Redundant Sources of Wnt Regulate Intestinal Stem Cells and Promote Formation of Paneth Cells. *Gastroenterology* **143**, 1518-1529.e7 (2012).
23. Aoki, R. *et al.* Foxl1-Expressing Mesenchymal Cells Constitute the Intestinal Stem Cell Niche. *Cell. Mol. Gastroenterol. Hepatol.* **2**, 175–188 (2015).
24. Degirmenci, B., Valenta, T., Dimitrieva, S., Hausmann, G. & Basler, K. GLI1-expressing mesenchymal cells form the essential Wnt-secreting niche for colon stem cells. *Nature* **558**, 449 (2018).
25. Greicius, G. *et al.* PDGFRα+ pericryptal stromal cells are the critical source of Wnts and RSPO3 for murine intestinal stem cells in vivo. *Proc. Natl. Acad. Sci.* **115**, E3173–E3181 (2018).
26. Kabiri, Z. *et al.* Stroma provides an intestinal stem cell niche in the absence of epithelial Wnts. *Development* **141**, 2206–2215 (2014).

27. Shoshkes-Carmel, M. *et al.* Subepithelial telocytes are an important source of Wnts that supports intestinal crypts. *Nature* **557**, 242–246 (2018).
28. Koslowski, M. J. *et al.* Association of a functional variant in the Wnt co-receptor LRP6 with early onset ileal Crohn's disease. *PLoS Genet.* **8**, e1002523 (2012).
29. Nava, P. *et al.* Interferon-γ Regulates Intestinal Epithelial Homeostasis through Converging β-Catenin Signaling Pathways. *Immunity* **32**, 392–402 (2010).
30. Eastwood, G. L. Gastrointestinal Epithelial Renewal. *Gastroenterology* **72**, 962–975 (1977).
31. Chen, M. & He, X. APC Deficiency Leads to β-Catenin Stabilization and Signaling Independent of LRP5/6. *Dev. Cell* **49**, 825–826 (2019).
32. Saito-Diaz, K. *et al.* APC Inhibits Ligand-Independent Wnt Signaling by the Clathrin Endocytic Pathway. *Dev. Cell* **44**, 566-581.e8 (2018).
33. Cabel, C. R. *et al.* Single-Cell Analyses Confirm the Critical Role of LRP6 for Wnt Signaling in APC-Deficient Cells. *Dev. Cell* **49**, 827–828 (2019).
34. East, J. E. *et al.* British Society of Gastroenterology position statement on serrated polyps in the colon and rectum. *Gut* **66**, 1181–1196 (2017).
35. Cagnol, S. & Rivard, N. Oncogenic KRAS and BRAF activation of the MEK/ERK signaling pathway promotes expression of dual-specificity phosphatase 4 (DUSP4/MKP2) resulting in nuclear ERK1/2 inhibition. *Oncogene* **32**, 564–576 (2013).
36. Bergeron, S. *et al.* The serine protease inhibitor serpinE2 is a novel target of ERK signaling involved in human colorectal tumorigenesis. *Mol. Cancer* **9**, 271 (2010).
37. Cooper, H. S., Murthy, S. N., Shah, R. S. & Sedergran, D. J. Clinicopathologic study of dextran sulfate sodium experimental murine colitis. *Lab. Investig. J. Tech. Methods Pathol.* **69**, 238–249 (1993).
38. Perreault, N., Sackett, S. D., Katz, J. P., Furth, E. E. & Kaestner, K. H. Foxl1 is a mesenchymal Modifier of Min in carcinogenesis of stomach and colon. *Genes Dev.* **19**, 311–315 (2005).
39. Leblanc, C. *et al.* Epithelial Src homology region 2 domain-containing phosphatase-1 restrains intestinal growth, secretory cell differentiation, and tumorigenesis. *FASEB J. Off. Publ. Fed. Am. Soc. Exp. Biol.* **31**, 3512–3526 (2017).
40. Gonneaud, A. *et al.* A SILAC-Based Method for Quantitative Proteomic Analysis of Intestinal Organoids. *Sci. Rep.* **6**, (2016).

41. Sato, T. *et al.* Long-term Expansion of Epithelial Organoids From Human Colon, Adenoma, Adenocarcinoma, and Barrett's Epithelium. *Gastroenterology* **141**, 1762–1772 (2011).
42. Wiederschain, D. *et al.* Single-vector inducible lentiviral RNAi system for oncology target validation. *Cell Cycle* **8**, 498–504 (2009).
43. Babeu, J.-P., Jones, C., Geha, S., Carrier, J. C. & Boudreau, F. P1 promoter-driven HNF4α isoforms are specifically repressed by β-catenin signaling in colorectal cancer cells. *J. Cell Sci.* **131**, (2018).
44. Bian, B. *et al.* Cathepsin B promotes colorectal tumorigenesis, cell invasion, and metastasis. *Mol. Carcinog.* **55**, 671–687 (2016).

Acknowledgements

We thank Pr Claude Asselin for critical reading of the manuscript. We thank the RNomics and Electron Microscopy & Histology Platforms of the FMSS at Université de Sherbrooke for services. Special thanks to Dr Martin McMahon (University of Utah) for providing the plasmid encoding the inducible $BRAF^{V600E}$:ER fusion protein. This research was supported by a grant from Canadian Institutes of Health Research (CIHR) to Nathalie Rivard. Jennifer Raisch holds a scholarship from the FRQS-Funded Centre de recherche du CHUS. Nathalie Rivard is a recipient of a Canadian Research Chair in colorectal cancer and inflammatory cell signaling.

Author contribution

JR performed most of the experiments. ACB, MJL and CL contributed to experiments. MJL also contributed to the histological analyses. JR and NR designed the experiments. JR, MJL and NR wrote the paper. NR was in charge of overall direction. All authors have read and approved the final manuscript.

Additional Information – Competing interest statement

The authors declare no conflicts of interest.
The study was carried out in compliance with the ARRIVE guidelines.

Figure legends

Figure 1: Loss of LRP6 expression does not alter intestinal architecture but affects Wnt target gene expression. (**a**) Loss of LRP6 expression and β-catenin levels were analyzed in small intestinal epithelial cell enriched lysates from 12-week-old mice by western blot. (**b**) Relative expression levels of Wnt/β-catenin target genes were evaluated by qPCR on intestinal epithelial cell enrichments from mutant mice compared to littermate controls ($n \geq 5$). (**c**) Villus length and crypt depth were determined on H&E stained jejunal sections ($n = 8$). Scale bars, 100 µm. (**d**) Proliferative cells were observed by BrdU immunohistochemistry on jejunal sections of mutant mice compared with control littermates ($n = 9$). Scale bars, 50 µm. (**e**) Relative expression of mucin 2 (*Muc2*), lysozyme (*Lyz1*) and sucrase-isomaltase (*Sis*), the main markers of respectively goblet, Paneth and absorptive differentiated cells, was evaluated by qPCR on intestinal epithelial cell enriched RNA ($n \geq 8$). (**f**) Immunofluorescence against OLFM4 (green) was performed on jejunal sections of 12-week-old controls and *Lrp6*$^{IEC\text{-}KO}$ mice ($n = 3$) to visualize intestinal stem cells. Scale bars, 50 µm. Data are expressed as mean ± SD. Mann-Whitney U test * $p \leq 0.05$, ** $p \leq 0.01$.

Figure 2: Enteroid development is impaired by loss of LRP6 expression. (**a**) Phase contrast images of enteroids 1-, 3- and 5-days after seeding. Scale bars, 50 µm. Protrusions per enteroid were counted 5-days after seeding ($n = 6$). Chi square, ***$p \leq 0.001$. (**b**) Enteroid proliferation was evaluated 3-days after seeding by EdU incorporation followed by immunofluorescence ($n = 4$). Scale bars, 50 µm. Unpaired t-test, *$p \leq 0.05$. (**c**) Enteroid viability was determined 5-days after seeding by phase contrast microscopy ($n = 3$). Unpaired t-test, *$p \leq 0.05$. (**d**) and (**e**) *Noxa*, *Ascl2*, *Lgr5*, *Axin2* and *Cd44* expression was evaluated by qPCR of RNA isolated from mutant enteroids compared to controls, 3-days after seeding ($n \geq 3$), Unpaired t-test, *$p \leq 0.05$. (**f**) Enteroid LRP6 expression was analyzed by western blot 3-days after seeding.

Figure 3: *Lrp6*$^{IEC\text{-}KO}$ mice are more sensitive to DSS-induced colitis. Ten to twelve-week-old *Lrp6*$^{IEC\text{-}KO}$ mice and their control littermates were treated with 1,75-2% DSS in drinking water for 7 days. (**a**) Body weight was measured every day during treatment ($n = 18$). (**b**) Disease activity index of *Lrp6* knockout mice and control littermates was calculated by scoring stool softness, occult fecal blood, rectal bleeding and colon rigidity at sacrifice ($n \geq 15$). (**c**) and (**d**) Hematoxylin

and eosin staining was performed on *Lrp6*$^{IEC\text{-}KO}$ and control colon tissues to score damage (**c**) according to the extent of mucosal architecture destruction, immune cell infiltration, Goblet cell depletion, muscle thickening and crypt abscesses ($n \geq 15$). Scale bars, 100 µm. Data are expressed as mean ± SEM. Mann-Whitney U test; *$p \leq 0.05$.

Figure 4: LRP6 downregulation does not affect adenoma formation in *Apc*$^{Min/+}$ mice and growth of colorectal cancer cells. (**a**) Polyp number was counted in 12-week-old *Lrp6*$^{loxP/loxP}$;*Villin*-Cre;*Apc*$^{Min/+}$ small intestines compared to controls (*Lrp6*$^{loxP/+}$;*Apc*$^{Min/+}$ or *Lrp6*$^{loxP/loxP}$;*Apc*$^{Min/+}$) ($n \geq 5$). (**b**) Small intestinal polyp size (diameter) was analyzed in *Lrp6*$^{loxP/loxP}$;*Villin*-Cre;*Apc*$^{Min/+}$ and control mice ($n \geq 5$). (**c**) Expression of a shRNA against *LRP6* (shLRP6) or a non-target shRNA (shCTRL) was induced with 50 ng/ml doxycycline for 48 h in HCT116 and SW48 cells. Loss of LRP6 expression was determined by western blot. (**d**) shLRP6 or shCTRL expression was induced with 50 ng/ml doxycycline 48 h before cells were seeded at low density to perform a clonogenic assay. Cells were grown for 14 days before staining with crystal violet and colonies were counted ($n = 3$). (**e**) and (**f**) shLRP6 or shCTRL expression was induced with 50 ng/ml doxycycline 48 h before soft agar seeding. HCT116 cells were grown for 14 days and SW48 cells for 21 days in soft agar before MTT staining. The number of colonies (**e**) and their size (**f**) were evaluated ($n = 3$). Data are expressed as mean ± SD.

Figure 5: LRP6 is phosphorylated in an ERK-dependent manner in human KRAS or BRAF mutated colorectal cancer cell lines and plays a role in BRAF-induced tumorigenic potential of intestinal epithelial cells. (**a**) HCT116 (mutated for *KRAS*), HT-29 (mutated for *BRAF*), Caco-2/15 and SW48 cells (both wild-type for *KRAS* and *BRAF*) were treated with SCH772984 (1 µM) or DMSO in fresh medium for 1 h and 6 h. Protein expression and phosphorylation were analyzed by western blot. (**b**) Loss of LRP6 expression was determined by western blot in IEC-6 cells transformed by the inducible BRAF^{V600E}:ER fusion protein and stably expressing a shRNA against *Lrp6* (shLrp6) or a control shRNA (shCtrl) compared to non-transfected cells. (**c**) IEC6 BRAF^{V600E}:ER cells stably expressing a shRNA against *Lrp6*, a control shRNA or non-transfected were treated with 250 nM 4OH-tamoxifen 16 h before soft agar seeding. Cells were grown for 3-5 weeks in soft agar before MTT staining. The number of colonies was evaluated ($n = 3$). Data are expressed as mean ± SD. Paired t-test, **$p \leq 0.01$.

Figures

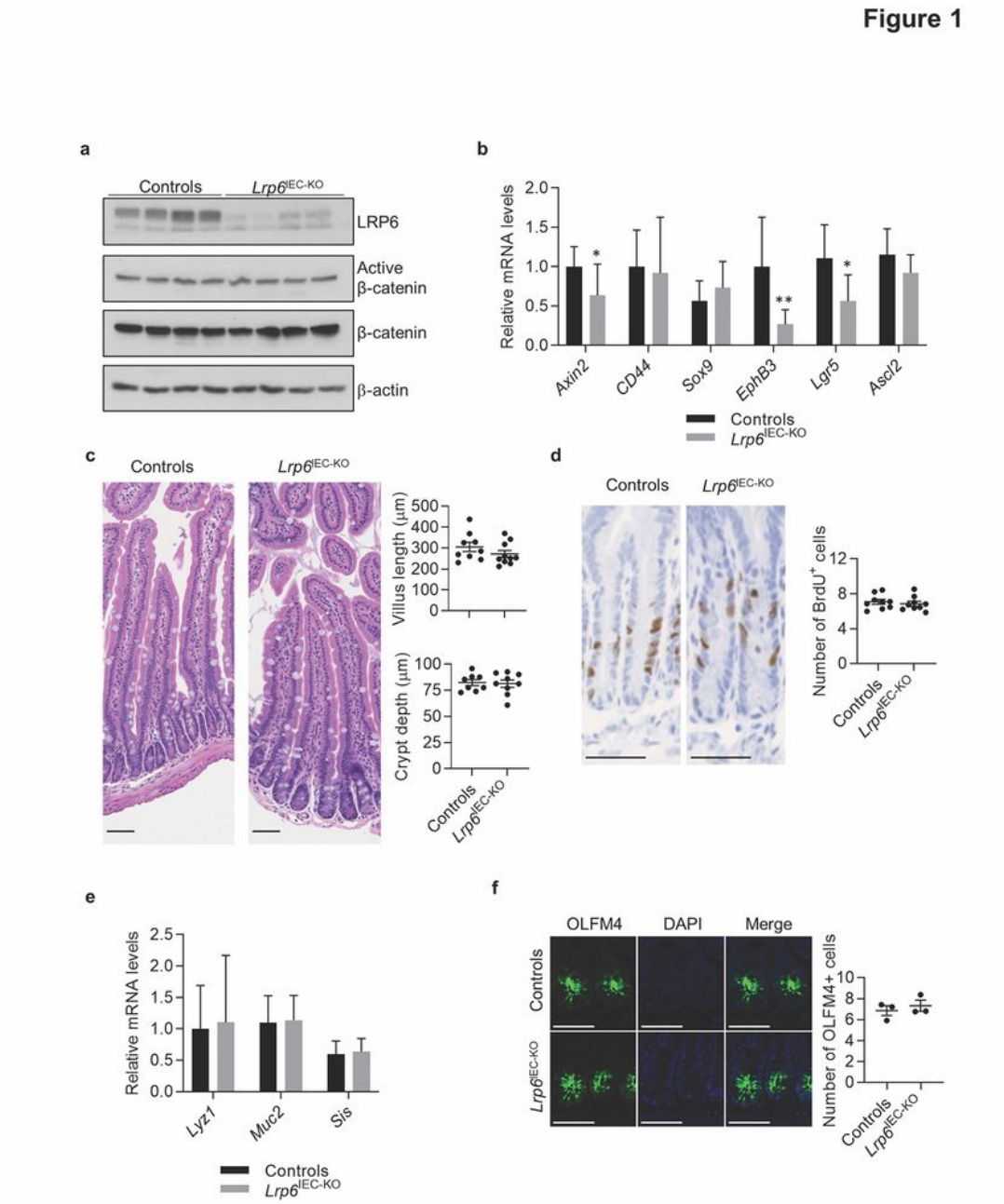

Figure 1

Loss of LRP6 expression does not alter intestinal architecture but affects Wnt target gene expression. (a) Loss of LRP6 expression and β-catenin levels were analyzed in small intestinal epithelial cell enriched lysates from 12-week-old mice by western blot. (b) Relative expression levels of Wnt/b-catenin target

genes were evaluated by qPCR on intestinal epithelial cell enrichments from mutant mice compared to littermate controls (n ≥ 5). (c) Villus length and crypt depth were determined on H&E stained jejunal sections (n = 8). Scale bars, 100 μm. (d) Proliferative cells were observed by BrdU immunohistochemistry on jejunal sections of mutant mice compared with control littermates (n = 9). Scale bars, 50 μm. (e) Relative expression of mucin 2 (Muc2), lysozyme (Lyz1) and sucrase-isomaltase (Sis), the main markers of respectively goblet, Paneth and absorptive differentiated cells, was evaluated by qPCR on intestinal epithelial cell enriched RNA (n ≥ 8). (f) Immunofluorescence against OLFM4 (green) was performed on jejunal sections of 12-week-old controls and Lrp6IEC-KO mice (n = 3) to visualize intestinal stem cells. Scale bars, 50 μm. Data are expressed as mean ± SD. Mann-Whitney U test * $p \leq 0.05$, ** $p \leq 0.01$.

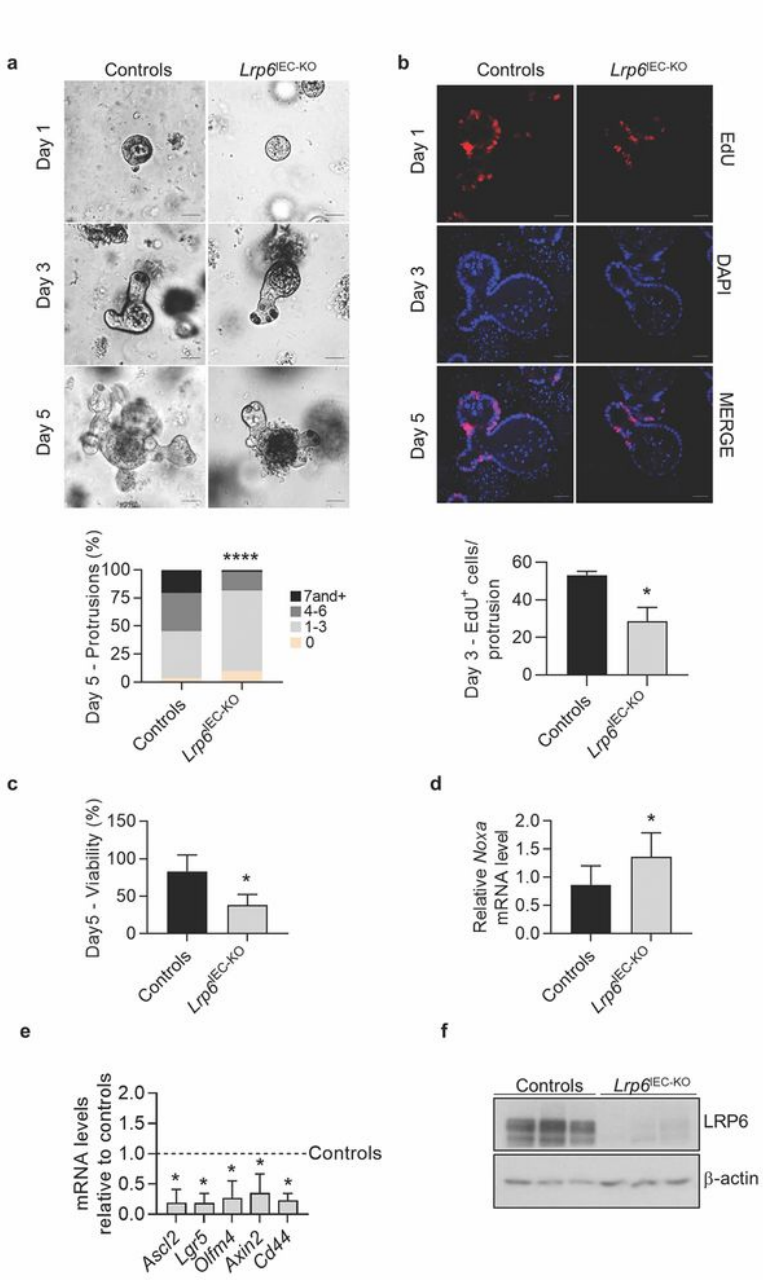

Figure 2

Enteroid development is impaired by loss of LRP6 expression. (a) Phase contrast images of enteroids 1-, 3- and 5-days after seeding. Scale bars, 50 µm. Protrusions per enteroid were counted 5-days after seeding (n = 6). Chi square, ***p ≤ 0.001. (b) Enteroid proliferation was evaluated 3-days after seeding by EdU incorporation followed by immunofluorescence (n = 4). Scale bars, 50 µm. Unpaired t-test, *p ≤ 0.05. (c) Enteroid viability was determined 5-days after seeding by phase contrast microscopy (n = 3). Unpaired

t-test, *p ≤ 0.05. (d) and (e) Noxa, Ascl2, Lgr5, Axin2 and Cd44 expression was evaluated by qPCR of RNA isolated from mutant nteroids compared to controls, 3-days after seeding (n ≥ 3), Unpaired t-test, *p ≤ 0.05. (f) Enteroid LRP6 expression was analyzed by western blot 3-days after seeding.

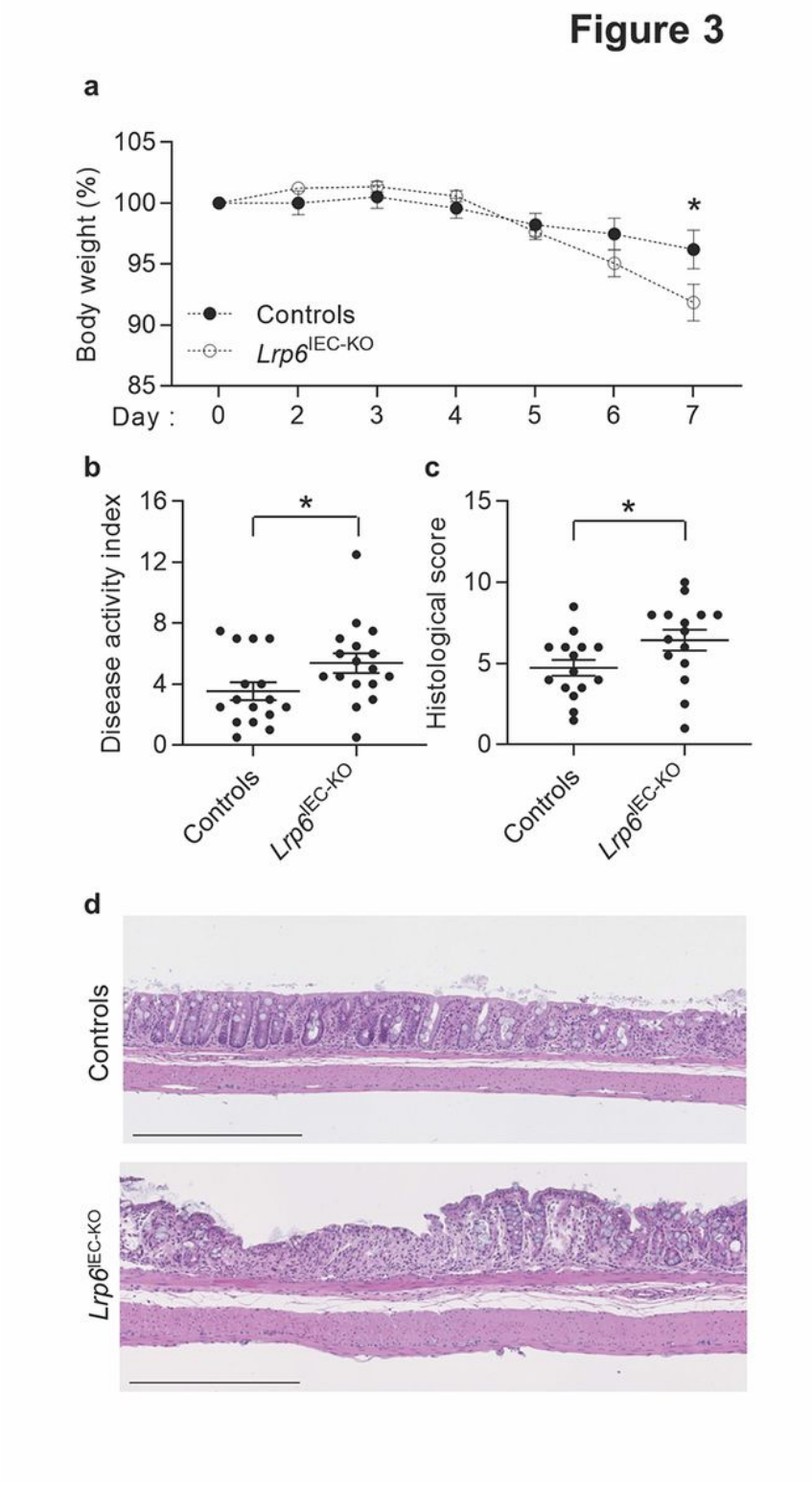

Figure 3

Lrp6IEC-KO mice are more sensitive to DSS-induced colitis. Ten to twelve-week-old Lrp6IEC-KO mice and their control littermates were treated with 1,75-2% DSS in drinking water for 7 days. (a) Body weight was

measured every day during treatment (n = 18). (b) Disease activity index of Lrp6 knockout mice and control littermates was calculated by scoring stool softness, occult fecal blood, rectal bleeding and colon rigidity at sacrifice (n ≥ 15). (c) and (d) Hematoxylin and eosin staining was performed on Lrp6IEC-KO and control colon tissues to score damage (c) according to the extent of mucosal architecture destruction, immune cell infiltration, Goblet cell depletion, muscle thickening and crypt abscesses (n ≥ 15). Scale bars, 100 μm. Data are expressed as mean ± SEM. Mann-Whitney U test; *p ≤ 0.05.

Figure 4

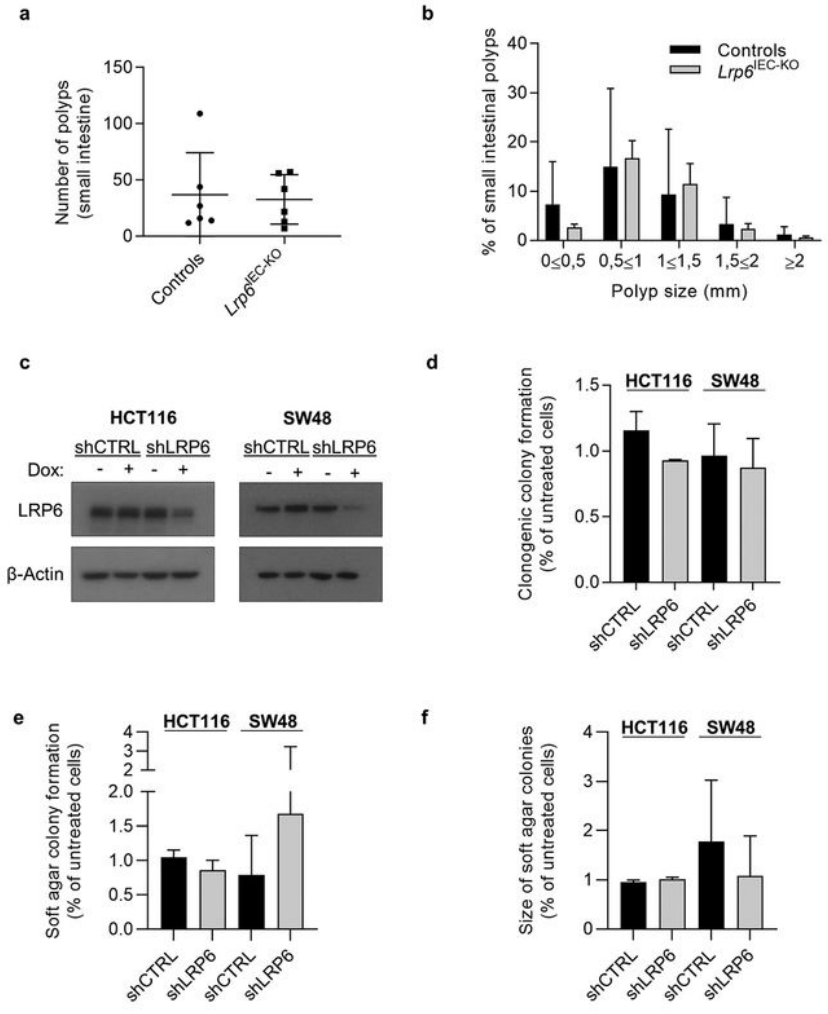

Figure 4

LRP6 downregulation does not affect adenoma formation in ApcMin/+ mice and growth of colorectal cancer cells. (a) Polyp number was counted in 12‐week‐old Lrp6loxP/loxP;Villin-Cre;ApcMin/+ small intestines compared to controls (Lrp6loxP/+;ApcMin/+ or Lrp6loxP/loxP;ApcMin/+) (n ≥ 5). (b) Small intestinal polyp size (diameter) was analyzed in Lrp6loxP/loxP;Villin-Cre;ApcMin/+ and control mice (n ≥ 5). (c) Expression of a shRNA against LRP6 (shLRP6) or a non-target shRNA (shCTRL) was induced with 50 ng/ml doxycycline for 48 h in HCT116 and SW48 cells. Loss of LRP6 expression was determined by western blot. (d) shLRP6 or shCTRL expression was induced with 50 ng/ml doxycycline 48 h before cells were seeded at low density to perform a clonogenic assay. Cells were grown for 14 days before staining with crystal violet and colonies were counted (n = 3). (e) and (f) shLRP6 or shCTRL expression was induced with 50 ng/ml doxycycline 48 h before soft agar seeding. HCT116 cells were grown for 14 days and SW48 cells for 21 days in soft agar before MTT staining. The number of colonies (e) and their size (f) were evaluated (n = 3). Data are expressed as mean ± SD.

Figure 5

LRP6 is phosphorylated in an ERK-dependent manner in human KRAS or BRAF mutated colorectal cancer cell lines and plays a role in BRAF-induced tumorigenic potential of intestinal epithelial cells. (a) HCT116 (mutated for KRAS), HT-29 (mutated for BRAF), Caco-2/15 and SW48 cells (both wild-type for KRAS and BRAF) were treated with SCH772984 (1 μM) or DMSO in fresh medium for 1 h and 6 h. Protein expression and phosphorylation were analyzed by western blot. (b) Loss of LRP6 expression was determined by

western blot in IEC-6 cells transformed by the inducible BRAFV600E:ER fusion protein and stably expressing a shRNA against Lrp6 (shLrp6) or a control shRNA (shCtrl) compared to non-transfected cells. (c) IEC6 BRAFV600E:ER cells stably expressing a shRNA against Lrp6, a control shRNA or non-transfected were treated with 250 nM 4OH-tamoxifen 16 h before soft agar seeding. Cells were grown for 3-5 weeks in soft agar before MTT staining. The number of colonies was evaluated (n = 3). Data are expressed as mean ± SD. Paired t-test, **p ≤ 0.01.

Supplementary Files

This is a list of supplementary files associated with this preprint. Click to download.

- SupplementaryMaterial.pdf